07ICES-92

Numerical Uncertainty Quantification for Radiation Analysis Tools

Brooke Anderson, Steve Blattnig, Martha Clowdsley
NASA Langley Research Center

ABSTRACT

Recently a new emphasis has been placed on engineering applications of space radiation analyses and thus a systematic effort of Verification, Validation and Uncertainty Quantification (VV&UQ) of the tools commonly used for radiation analysis for vehicle design and mission planning has begun. There are two sources of uncertainty in geometric discretization addressed in this paper that need to be quantified in order to understand the total uncertainty in estimating space radiation exposures. One source of uncertainty is in ray tracing, as the number of rays increase the associated uncertainty decreases, but the computational expense increases. Thus, a cost benefit analysis optimizing computational time versus uncertainty is needed and is addressed in this paper. The second source of uncertainty results from the interpolation over the dose vs. depth curves that is needed to determine the radiation exposure. The question, then, is what is the number of thicknesses that is needed to get an accurate result. So convergence testing is performed to quantify the uncertainty associated with interpolating over different shield thickness spatial grids.

INTRODUCTION

Astronaut risk due to radiation exposure is often expressed in terms of dosimetric quantities such as dose and dose equivalent. To calculate these quantities, the radiation environment at one or more points inside a human body within a space vehicle must be calculated. A number of tools and/or models exist for this purpose including external radiation environments models, vehicle shielding models, human body geometry models, ray tracing codes, and radiation transport codes.

The analysis described in this paper is performed using a radiation analysis tool set under development at NASA Langley Research Center. This tool set utilizes the 2005 version of the HZETRN space radiation transport code, which is described in greater detail later in the paper. The process begins with an external radiation environment model containing an energy spectrum for each type of particle found in the environment. This environment is altered by the materials making up the vehicle and the human body itself. Charged ions lose energy due to ionization, and nuclear collisions occur, producing secondary ions as well as neutrons. The HZETRN code is used to calculate these changes in radiation environment for the appropriate shield materials.

An accurate determination of the amount of material that is between the target location and the external source of the radiation is crucial. This amount is calculated by applying a ray tracing methodology to the vehicle and/or human body model. This ray tracing determines the amount of material along each of a large number of rays originating at the target location. Here, the questions of how many rays are needed and how they should be distributed over 4π steradian become very important. In some instances, it is important to make sure that each ray subtends the same solid angle. Numerous ray distributions have been used in the past and present, with the number of rays ranging from 512 to 4002. As the number of rays increase the associated uncertainty decreases, but the computational expense increases. Thus, a cost benefit analysis optimizing computational time versus uncertainty is needed and is addressed in this paper.

To save computation time, rather than calculating the radiation transport for each ray in the ray trace, dosimetric quantities are sometimes calculated for several shielding material thicknesses and then interpolation is used to evaluate intermediate quantities. This option is especially desirable early in the design process when the vehicle is constantly being altered. Then the question is, what is the number of thicknesses that are needed to get an accurate result.

In this paper, the uncertainty resulting from ray tracing the same location using different ray distributions is examined. This analysis is performed for two different habitats with CAD models of varying complexity. This

analysis is performed for two radiation environments: a free-space galactic cosmic ray (GCR) environment and the August 1972 solar particle event (SPE). Note that these environments are not appropriate environments for the habitats modeled, since lunar surface effects are not considered. The charged ion environment on the lunar surface is approximately half that of free-space due to the moon's shadow. In addition, the lunar surface environment contains a neutron component resulting from interactions between the free-space charged ions and the lunar regolith. Convergence testing is also performed to quantify the uncertainty associated with interpolating over the dose vs. shield thickness data of varying fidelity. For these analyses, dose and dose equivalent in tissue were calculated, but human body models were not utilized. The scripts used for this study, as well as the results, have been stored in the radiation analysis tool environment, so that these calculations can be reproduced as the tools are improved.

VEHICLES/HABITATS CAD MODELS

LUNAR LANDER

The lunar lander model (figure 1) is part of the Gateway Scenario [1]. Its purpose is to transport crew between the Gateway station and the lunar surface. It is designed for a 9-day mission, with a 3-day stay on the lunar surface. The model consists of 26 components, with most of the components being the descent/ascent engine, propellant, and small crew quarters that includes an ECLSS system.

Figure 1. Outside view of the Lunar Lander.

LUNAR HABITAT

The lunar habitat (figures 2 and 3) is designed to be a 30 days surface habitat and science laboratory for a crew of four at the lunar South Pole [1]. It was designed to provide crew accommodations and lab support for surface missions, along with providing airlocks for crew EVA and radiation protection. The habitat is capable of autonomous landing and system startup following the landing. It also provides support to the unpressurized rovers and survival power to a dormant L1 Lunar Lander. The facility consists of three levels with a total pressurized volume of 240 m^3. It has an outer diameter of 6.5 meters and an inner diameter 6.0 meters. The lowest level houses two two-person airlocks, which can also act as shelters during solar particle events. It also contains an unpressurized porch that crewmembers may use to dust off prior to vehicle ingress. The second deck contains the science laboratory and the mechanical and avionics systems. The third floor houses the crew quarters, galley and wardroom. The core structure consists of the pressure vessel and aft skirt along with Micro-Meteoroid Object Debris (MMOD) protection that also serves as the primary structure and integral shroud during launch. The core structure is designed to be a cylindrical pressure vessel at 70.33 kPa internal pressure and is approximately 6 meters tall by 6 meters in diameter. It was designed to have a 5-year lifetime.

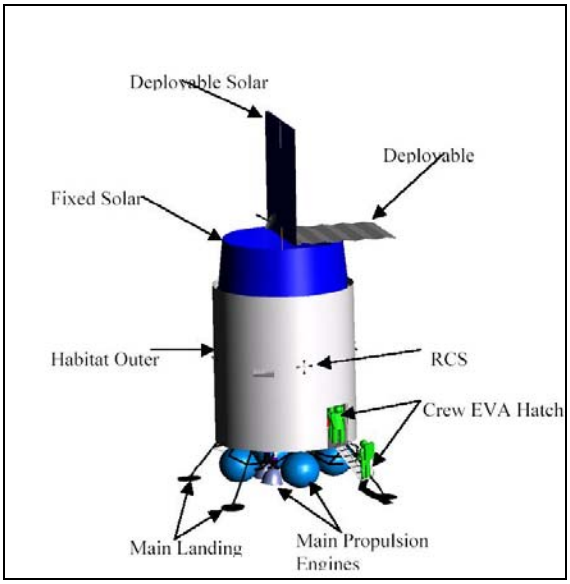

Figure 2. Outside view of the Lunar Habitat.

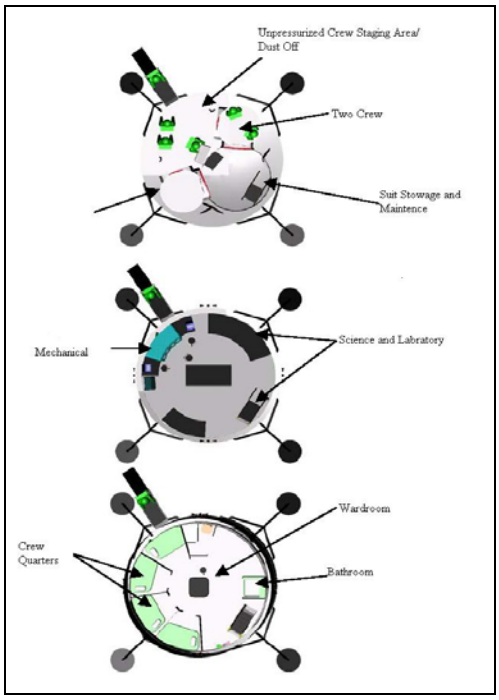

Figure 3. Inside view of the Lunar Habitat.

MODELING OF THE VEHICLES

Modeling for all the vehicles was done in the commercial CAD package I-DEAS. The original models, coming from both Langley Research Center and Johnson Space Center, had to be modified to make sure every part had a well-defined volume and mass and to simplify the models to allow for quicker calculations. The number of components for these vehicles is between 26 and 40. Once the solid model was complete, a Finite Element Model (FEM) was generated. The FEM discretization was selected manually by choosing the number of nodes/elements to be applied at the vertices. This is done to give a cleaner FEM and to make sure the number of elements/nodes was kept to a minimum to allow for more high-speed calculations while preserving the integrity of the shield model. The total number of elements for these two models is 4,000 for the lander and 15,000 for the habitat. For this analysis, two target points were run for each of the vehicles/habitats. The target points were chosen to represent places that provided both large and small amounts of shielding due to structure, storage, and equipment. The thickness distributions of these target points for the two models are shown in Figure 4.. Also it is assumed that most of the components within these vehicles are comprised of aluminum, thus the only material used in the transport analysis was aluminum and non-aluminum elements were scaled by the ratio of their density to that of aluminum.

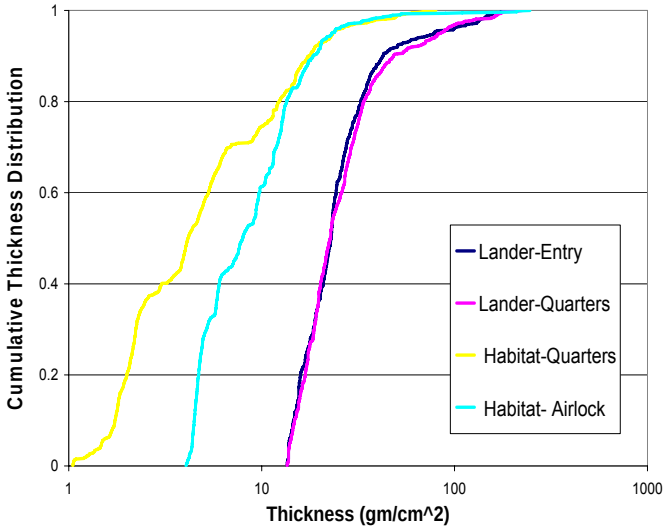

Figure 4. Thickness Distributions of models.

RAYTRACING

To calculate the radiation environment at a given point in the habitat using HZETRN 2005 (described below), the habitat shielding model must be "ray-traced." This "raytracing" is performed by dividing the volume surrounding the target point into a number of equal solid angles and calculating the thickness of each type of shielding along a ray through each solid angle. HZETRN 2005 can then be used to calculate the transport of the external environment through the material thicknesses along each ray. In the past the 512 and 968 ray distributions were used (see figure 5). The problem with these ray distributions is that there is a hole at the top and bottom of the sphere, so more recently a 970 ray distribution was used in which the hole was capped. Other ray distributions used more recently are the 1922 and 4002 ray sets (see figure 6), which have no gaps at the top or bottom of the sphere. All of these sets are analyzed to see how the spheres with holes affect the results and how increasing number of rays decreases the error.

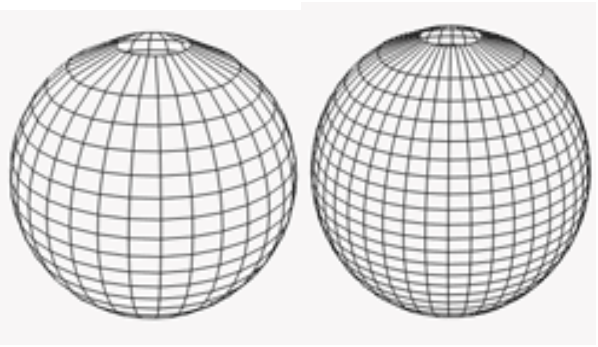

Figure 5. 512 and 968 Ray Distributions.

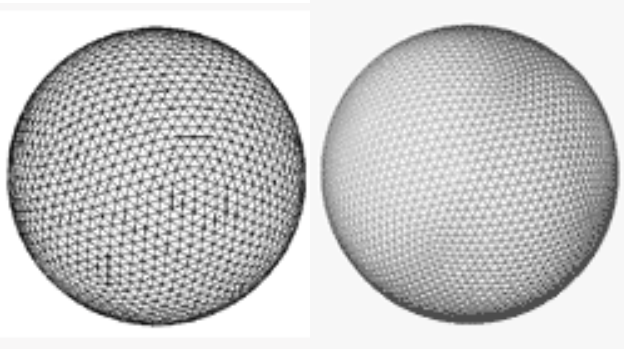

Figure 6. 1922 and 4002 Ray Distributions.

SPACE ENVIRONMENTS

The first requirement for evaluating space radiation exposure risk is an accurate description of the radiation environment outside the vehicle or habitat. This description should include an energy spectrum for each type of particle found in the environment. In free space, there are two types of environments of concern: galactic cosmic rays (GCR) and large solar particle events (SPE).

The galactic cosmic rays (GCR) consist of high energy atomic nuclei of the elements of composition roughly corresponding to their observed natural abundance. Hence, protons are most abundant, but the contributions to exposure from heavier elements (e.g., C, O, Si, and Fe) are notably significant in that their greater mass, charge and energy offset their lower flux in interactions with condensed matter. The GCR are always present, with flux values about 3 times greater at solar minimum than at solar maximum. In the absence of large flare activity, the GCR will dominate the exposure in free-space. These particles, and especially their high energy secondaries, are capable of penetrating very thick shields, and some degree of exposure is practically unavoidable. For this study, the 1977 solar minimum GCR environment was modeled using the particle spectra for protons, helium ions, carbon ions, oxygen ions, silicon ions, and iron ions predicted by the Badhwar-O'neill model updated in 2004 [2]. The spectra for the other ions with charge 1 through 28 are modeled by scaling from the previously mentioned ions using the CRÈME model. [3] The CRÈME model is still used because we haven't fully updated our software. In the future, we will drop the CRÈME scaling and just use the ONeil model. In general, the particle flux correlates with observed cosmic elemental abundance. The differential flux vs. energy for some of the more important GCR ions is plotted in Figure 7.

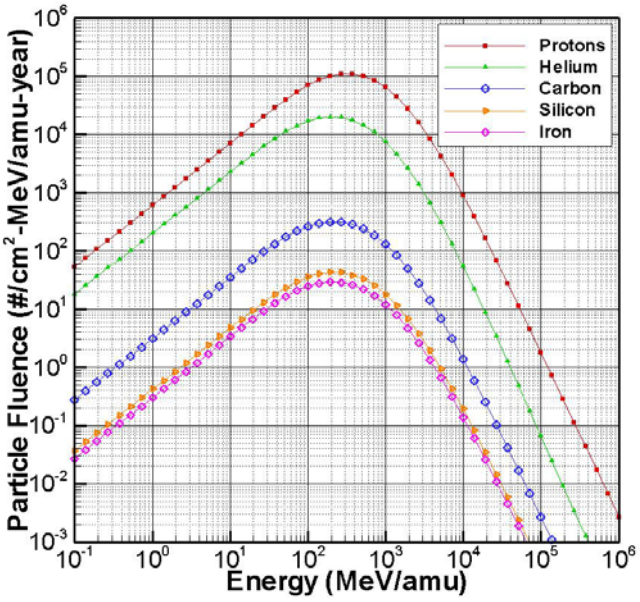

Figure 7. Particle Flux for GCR.

Large solar particle events are rare, isolated events with durations usually measured in hours. Solar particle events occur when a large number of particles, mostly protons, move through the solar system. These events usually happen during periods of increased solar activity and appear to correspond to large coronal mass ejections [4]. The flare spectrum selected for this study is that of August 1972 event as modeled by J. King [5], shown in Figure 8. The King spectrum is modeled using the equation: $_{p}=2.98\text{x}10^{8}e^{-(E-30/26.5)}$. It is noteworthy that this particular flare erupted within months of the flights of Apollo XVI and XVII – Apr. and Dec. 1972. Although such flares are rare, their hazard is great since an occurrence during a lunar or Mars mission could adversely affect mission operations.

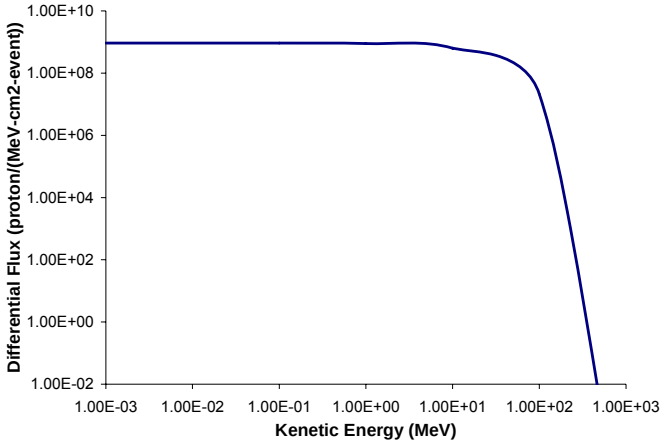

Figure 8. Differential Flux for SPE

TRANSPORT

The high-charge-and energy (HZE) transport computer program HZETRN [6] was developed to address the problems of space radiation transport and shielding. The HZETRN2005 program was intended specifically for the design engineer who is interested in obtaining fast and accurate dosimetric information for the design of space modules and devices. The code is a versatile and efficient deterministic program that solves the set of coupled linear Boltzmann transport equations for fluences $\phi_j(\mathbf{x},\mathbf{\Omega},E)$ of type-j particles of energy E at location **x**:

$$\vec{\Omega} \bullet \nabla \phi_j(\vec{x},\vec{\Omega},E) + \sigma_j(E)\phi_j(\vec{x},\vec{\Omega},E) = \sum \int \sigma_{j,k}(\vec{\Omega},\vec{\Omega}',E,E')\phi_k(\vec{x},\vec{\Omega}',E')d\vec{\Omega}'\,dE' \quad (1)$$

where σ_j is the macroscopic cross section for removal of type *j* particles with energy *E* in the target medium and σ_{jk} represents processes for which type k particles moving in direction **Ω′** with energy E′ produce a type j particle moving in direction **Ω** with energy E including decay processes. This code uses a "straight ahead" approximation in which it is assumed that all secondary particles move in the same directions as the primaries. This approximation reduces the Boltzmann equation to:

$$[\partial x - Aj\text{-}1\partial E\, Sj(E) + \sigma j(E)]\, \varphi j(x,E) = \Sigma \int \sigma jk(E,E')\, \varphi k(x,E')\, dE' \quad (2)$$

where *Aj* is the atomic weight of type *j* particles and S*j* is the stopping power for type *j* particles. This equation is then solved using a marching technique. In this way, the particle fluence spectra can be calculated at any depth in any shielding material.

In addition to fluence spectra, the HZETRN code will calculate dose and dose equivalent. Dose is the energy absorbed per unit mass of material or tissue and is measured in grays (1 Gy = 100 rad = 1 J per kg). Some types of particles are more damaging to human tissue than others. For this reason, dose equivalent was developed and defined as

$$H = \int Q(L)D(L)dL \quad (3)$$

where *L* is the linear energy transfer and *Q* is a quality factor. HZETRN2005 utilizes the quality factor recommended in the International Commission for Radiological Protection (ICRP) report no. 60 [7] and adopted by the National Council on Radiation Protection and Measurements (NCRP) [8] given by

$$\begin{aligned} Q(L) &= 1, && L < 10 \\ Q(L) &= 0.32L - 2.2, && 10 < L < 100 \\ Q(L) &= 300L^{-1/2}, && L < 100 \end{aligned} \quad (4)$$

where the linear energy transfer, L, is in keV/μm and dose equivalent is in sieverts (1 Sv = 100 rems).

Dose equivalent versus shield thickness curves for Aluminum for the 1977 solar minimum GCR environment and the August 1972 (King spectrum) SPE environment are shown in figures 9 and 10, respectively, for three different spatial grids. Note the differences in scale on the y-axis of these plots showing that for the SPE environment, small changes in shield thickness can result in large changes in exposure.

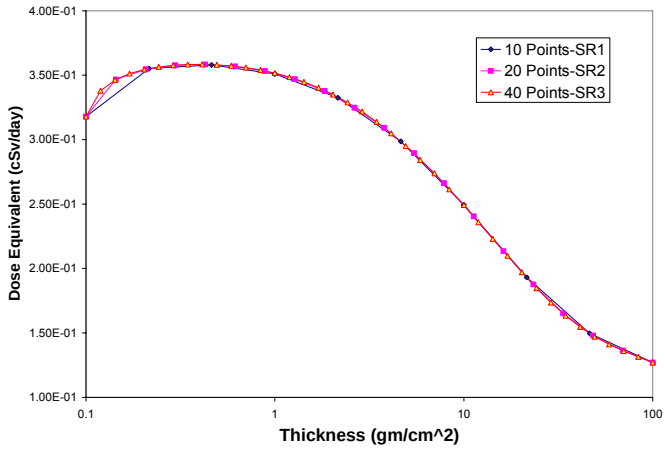

Figure 9. GCR Dose Equivalent vs. Depth for Aluminum.

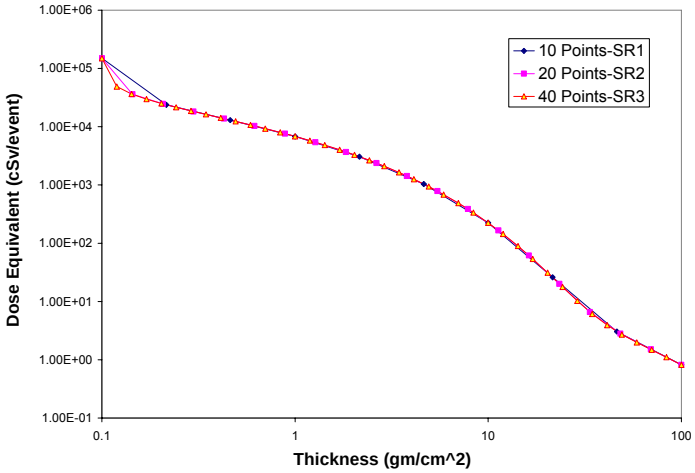

Figure 10. SPE Dose Equivalent vs. Depth for Aluminum.

SPATIAL GRIDS FOR INTERPOLATION

As was stated in the introduction, dosimetric quantities are sometimes calculated for several shielding material thicknesses and then this data is interpolated over in order to save computational time. As with the ray tracing, the more data points lead to increased accuracy at the expense of computational time. Three spatial grids were used, ranging from 0.1 gm/cm^2 of aluminum to 100 gm/cm^2. The grid points were equally spaced on a log scale. The first grid has ten points, the second grid uses 20 points, and the third grid uses 40 points. The 10 point spatial grid is approximately equivalent to what has often been used for calculations using HZETRN in the past.

RESULTS AND CONCLUSIONS

Dose and dose equivalent values for each of the target locations in the two habitats for both GCR and SPE environments are given in Tables 1 – 12 in the appendix.

The results in Tables 1-12 show that a significant increase in accuracy is not achieved by using more than 512 rays for GCR calculations. Based on these results we conclude that for thickness distributions similar to those given in figure 4, a 512 ray distribution is sufficient for GCR calculations and will result in numerical error of less that one percent. For SPE calculations, differences on the order of one percent and not more than four percent are seen and the results are not always smoothly converging as the number of rays is increased. These results differ from the GCR in this manner because SPE exposure is more sensitive to shield thickness as shown in figures 9 and 10. The lack of smooth convergence may be due to the qualitative differences in the geometric layout in the different ray distributions. However, all five ray distributions give approximately the same results with differences much less than the physical uncertainties of approximately 10% estimated by Cucinotta, et al. [9]. For most purposes, any of the ray distributions are sufficient but it is recommended that for high consequence calculations, multiple ray distributions are run to ensure a reasonable representation of the geometry.

The results in Tables 13-16 show the percent difference between the first, 10-point spatial grid and the third, 40-point, spatial grid. Similarly, the results in tables 17-20 show the percent difference between the second 20-point spatial grid and the third, 40-point spatial grid. Since there is smooth convergence with very small difference between the second and third spatial grids, these differences are a good approximation to the numerical error due to having a discrete spatial grid. For the GCR results the error for the 10-point grid is less than one percent and is much less than the physical uncertainties. For SPE, the 10-point grid has large errors and it is recommended that it not be used in the future. The 20-point grid has errors less than once percent and is, therefore, deemed sufficient.

In summary, calculations have been performed for GCR and SPE free-space environments for four different vehicle geometries. All five different ray distributions gave approximately the same results. The 10 point spatial grid is sufficient for GCR calculations and the 20 point for SPE. For high consequence calculations, however, it is recommended that this type of convergence testing be repeated for the vehicle in question

REFERENCES

1. J. R. Geffre , “Conceptual Design of a Lunar L1 Gateway Outpost,” 34th COSPAR Scientific Assembly, The Second World Space Congress; Houston, TX, 2002
2. P. M. O’Neill, “Badhwar–O_Neill galactic cosmic ray model update based on advanced composition explorer (ACE) energy spectra from 1997 to present,” *Adv. Space Res.*, 37, pp. 1727-1733, 2006
3. J. H. Adams Jr., "Cosmic Ray Effects on Microelectronics, Part IV" NRL Memo report 5901
4. D. V. Reames, “Particle Acceleration at the Sun and in the Heliosphere,” *Space Sci. Rev.,* Vol. 90, nos. 3-4, pp. 413-491, 1999
5. Joseph H. King, “Solar Proton Fluences for 1977-1983 Space Missions,” *J. Spacecr. 8_ Rockets,* vol. 11, no. 6, pp. 401-408, 1974
6. J.W. Wilson, R.K. Tripathi, F.F. Badavi, and F.A. Cucinotta, “Standardized Radiation Shield Design Method: 2005 HZETRN,” presented at: International Conference on Environmental Systems; Norfolk, VA, 2006
7. “1990 Recommendations of the International Commission for Radiological Protection,” ICRP Report No. 60, Annuals of the ICRP 21, No. 1-3, Elsevier Science, 1991
8. “Limitation of Exposure to Ionizing Radiation,” NCRP Report No. 116, National Council on Radiation Protection and Measurements, Bethesda, MD, 1993
9. F. A. Cucinotta, et. al. "Managing Lunar and Mars Mission Radiation Risks Part I: Cancer Risks, Uncertainties and Shielding Effectiveness NASA TP-2005-213164 2005

CONTACT

Brooke Anderson Park at NASA Langley Research Center, brooke.m.anderson@nasa.gov

APPENDIX

Table 1. Dose and Dose Equivalent for the Lunar Lander, Crew Quarters, using 10 points for Spatial Resolution grid.

10 points-SR1

Model	Target Point	# of Rays	GCR-DOSE	GCR-DOSE EQUIV.	SPE-DOSE	SPE-DOSE EQUIV.
Lunar Lander	Quarters	512	0.0547	0.1856	16.2193	30.1569
		968	0.0548	0.1859	16.1876	30.1306
		970	0.0548	0.1856	16.0239	29.8581
		1922	0.0548	0.1855	15.8981	29.6491
		4002	0.0548	0.1855	15.8420	29.5677

Table 2. Dose and Dose Equivalent for the Lunar Lander, Entry, using 10 points for Spatial Resolution grid.

10 points-SR1

Model	Target Point	# of Rays	GCR-DOSE	GCR-DOSE EQUIV.	SPE-DOSE	SPE-DOSE EQUIV.
Lunar Lander	Entry	512	0.0551	0.1873	16.8048	31.2199
		968	0.0551	0.1876	17.0442	31.6338
		970	0.0551	0.1874	16.6699	31.0424
		1922	0.0551	0.1873	16.6769	31.0417
		4002	0.0551	0.1874	16.7346	31.1252

Table 3. Dose and Dose Equivalent for the Lunar Habitat, Airlock, using 10 points for Spatial Resolution grid.

10 points-SR1

Model	Target Point	# of Rays	GCR-DOSE	GCR-DOSE EQUIV.	SPE-DOSE	SPE-DOSE EQUIV.
Lunar Habitat	Left Airlock	512	0.0597	0.2575	298.3267	491.5811
		968	0.0596	0.2572	299.4854	493.5730
		970	0.0596	0.2574	300.7473	495.6469
		1922	0.0596	0.2577	304.6733	502.1139
		4002	0.0596	0.2577	304.6383	502.1039

Table 4. Dose and Dose Equivalent for the Lunar Habitat, Crew Quarters, using 10 points for Spatial Resolution grid.

10 points-SR1

Model	Target Point	# of Rays	GCR-DOSE	GCR-DOSE EQUIV.	SPE-DOSE	SPE-DOSE EQUIV.
Lunar Habitat	Quarters	512	0.0603	0.2854	1003.7660	1749.3550
		968	0.0604	0.2869	991.5247	1723.9580
		970	0.0604	0.2873	998.4348	1735.7850
		1922	0.0604	0.2881	1017.3980	1770.6140
		4002	0.0605	0.2888	1030.0760	1792.5460

Table 5. Dose and Dose Equivalent for the Lunar Lander, Crew Quarters, using 20 points for Spatial Resolution grid.

20 points-SR2

Model	Target Point	# of Rays	GCR-DOSE	GCR-DOSE EQUIV.	SPE-DOSE	SPE-DOSE EQUIV.
Lunar Lander	Quarters	512	0.0549	0.1856	17.4408	31.1234
		968	0.0550	0.1858	17.4061	31.0890
		970	0.0549	0.1855	17.2413	30.8119
		1922	0.0549	0.1854	17.1030	30.5910
		4002	0.0550	0.1855	17.0393	30.4998

Table 6. Dose and Dose Equivalent for the Lunar Lander, Entry, using 20 points for Spatial Resolution grid.

20 points-SR2

Model	Target Point	# of Rays	GCR-DOSE	GCR-DOSE EQUIV.	SPE-DOSE	SPE-DOSE EQUIV.
Lunar Lander	Entry	512	0.0552	0.1873	18.0689	32.1949
		968	0.0552	0.1876	18.3659	32.6537
		970	0.0552	0.1874	17.9638	32.0183
		1922	0.0552	0.1873	17.9676	32.0215
		4002	0.0552	0.1874	18.0309	32.1202

Table 7. Dose and Dose Equivalent for the Lunar Habitat, Airlock, using 20 points for Spatial Resolution grid.

20 points-SR2

Model	Target Point	# of Rays	GCR-DOSE	GCR-DOSE EQUIV.	SPE-DOSE	SPE-DOSE EQUIV.
Lunar Habitat	Left Airlock	512	0.0597	0.2582	304.1549	500.2024
		968	0.0597	0.2580	305.0261	501.7132
		970	0.0597	0.2581	306.3617	503.9023
		1922	0.0597	0.2584	310.5875	510.8587
		4002	0.0597	0.2585	310.5689	510.8666

Table 8. Dose and Dose Equivalent for the Lunar Habitat, Crew Quarters using 20 points for Spatial Resolution grid.

20 points-SR2

Model	Target Point	# of Rays	GCR-DOSE	GCR-DOSE EQUIV.	SPE-DOSE	SPE-DOSE EQUIV.
Lunar Habitat	Quarters	512	0.0603	0.2862	1019.9860	1775.0370
		968	0.0605	0.2877	1007.9340	1749.9320
		970	0.0604	0.2882	1014.7460	1761.6100
		1922	0.0605	0.2889	1033.4140	1795.9950
		4002	0.0605	0.2896	1046.2310	1818.1390

Table 9. Dose and Dose Equivalent for the Lunar Lander, Crew Quarters using 40 points for Spatial Resolution grid.

40 points-SR3

Model	Target Point	# of Rays	GCR-DOSE	GCR-DOSE EQUIV.	SPE-DOSE	SPE-DOSE EQUIV.
Lunar Lander	Quarters	512	0.0549	0.1855	17.7205	31.3229
		968	0.0550	0.1857	17.6779	31.2775
		970	0.0549	0.1854	17.5109	31.0001
		1922	0.0550	0.1853	17.3628	30.7692
		4002	0.0550	0.1853	17.3001	30.6754

Table 10. Dose and Dose Equivalent for the Lunar Lander, Entry using 40 points for Spatial Resolution grid.

40 points-SR3

Model	Target Point	# of Rays	GCR-DOSE	GCR-DOSE EQUIV.	SPE-DOSE	SPE-DOSE EQUIV.
Lunar Lander	Entry	512	0.0552	0.1871	18.3575	32.4027
		968	0.0552	0.1875	18.6324	32.8491
		970	0.0552	0.1872	18.2247	32.2041
		1922	0.0552	0.1872	18.2262	32.2036
		4002	0.0552	0.1872	18.2886	32.3012

Table 11. Dose and Dose Equivalent for the Lunar Habitat, Airlock using 40 points for Spatial Resolution grid.

40 points-SR3

Model	Target Point	# of Rays	GCR-DOSE	GCR-DOSE EQUIV.	SPE-DOSE	SPE-DOSE EQUIV.
Lunar Habitat	Left Airlock	512	0.0597	0.2582	306.8899	503.4977
		968	0.0597	0.2580	307.8790	505.1944
		970	0.0597	0.2581	309.1899	507.3449
		1922	0.0597	0.2584	313.3659	514.2129
		4002	0.0597	0.2585	313.3247	514.1965

Table 12. Dose and Dose Equivalent for the Lunar Habitat, Crew Quarters using 40 points for Spatial Resolution grid.

40 points-SR3

Model	Target Point	# of Rays	GCR-DOSE	GCR-DOSE EQUIV.	SPE-DOSE	SPE-DOSE EQUIV.
Lunar Habitat	Quarters	512	0.0604	0.2865	1025.1060	1785.4920
		968	0.0605	0.2880	1013.0450	1760.2820
		970	0.0605	0.2885	1019.9240	1772.1030
		1922	0.0605	0.2892	1038.7230	1806.7600
		4002	0.0606	0.2900	1051.6890	1829.2150

Table 13. Percent Difference between 10 Point Spatial Resolution and 40 Point Spatial Resolution for the Lunar Lander, Crew Quarters.

Model	Target Point	# of Rays	Percent Error GCR-Dose	Percent Error GCR-Dose Equiv.	Percent Error SPE-Dose	Percent Error SPE-Dose Equiv
Lunar Lander	Crew Quarters	512	0.3386	0.0903	8.4716	3.7223
		968	0.3044	0.0876	8.4304	3.6668
		970	0.3074	0.0872	8.4923	3.6839
		1922	0.3159	0.0932	8.4362	3.6404
		4002	0.3198	0.0965	8.4283	3.6108

Table 14. Percent Difference between 10 Point Spatial Resolution and 40 Point Spatial Resolution for the Lunar Lander, Entry.

Model	Target Point	# of Rays	Percent Error GCR-Dose	Percent Error GCR-Dose Equiv.	Percent Error SPE-Dose	Percent Error SPE-Dose Equiv
Lunar Lander	Entry	512	0.2818	0.0858	8.4580	3.6505
		968	0.2657	0.0827	8.5241	3.6994
		970	0.2751	0.0915	8.5316	3.6072
		1922	0.2790	0.0892	8.5002	3.6080
		4002	0.2842	0.0857	8.4971	3.6408

Table 15. Percent Difference between 10 Point Spatial Resolution and 40 Point Spatial Resolution for the Lunar Habitat, Airlock.

Model	Target Point	# of Rays	Percent Error GCR-Dose	Percent Error GCR-Dose Equiv.	Percent Error SPE-Dose	Percent Error SPE-Dose Equiv
Lunar Habitat	Left Airlock	512	0.1116	0.2941	2.7903	2.3668
		968	0.1158	0.2887	2.7263	2.3004
		970	0.1126	0.2864	2.7306	2.3057
		1922	0.1036	0.2959	2.7739	2.3529
		4002	0.1149	0.2974	2.7723	2.3517

Table 16. Percent Difference between 10 Point Spatial Resolution and 40 Point Spatial Resolution for the Lunar Habitat, Crew Quarters.

Model	Target Point	# of Rays	Percent Error GCR-Dose	Percent Error GCR-Dose Equiv.	Percent Error SPE-Dose	Percent Error SPE-Dose Equiv
Lunar Habitat	Quarters	512	0.1819	0.4114	2.0817	2.0239
		968	0.1853	0.4024	2.1243	2.0635
		970	0.1664	0.4070	2.1069	2.0494
		1922	0.1789	0.4032	2.0530	2.0006
		4002	0.1791	0.4022	2.0551	2.0046

Table 17. Percent Difference between 20 Point Spatial Resolution and 40 Point Spatial Resolution for the Lunar Lander, Crew Quarters.

Model	Target Point	# of Rays	Percent Error GCR-Dose	Percent Error GCR-Dose Equiv.	Percent Error SPE-Dose	Percent Error SPE-Dose Equiv
Lunar Lander	Crew Quarters	512	0.0264	0.0657	1.5786	0.6368
		968	0.0189	0.0692	1.5373	0.6026
		970	0.0182	0.0687	1.5396	0.6072
		1922	0.0215	0.0703	1.4963	0.5792
		4002	0.0232	0.0715	1.5076	0.5724

Table 18. Percent Difference between 20 Point Spatial Resolution and 40 Point Spatial Resolution for the Lunar Lander, Entry.

Model	Target Point	# of Rays	Percent Error GCR-Dose	Percent Error GCR-Dose Equiv.	Percent Error SPE-Dose	Percent Error SPE-Dose Equiv
Lunar Lander	Entry	512	0.0099	0.0755	1.5722	0.6413
		968	0.0016	0.0750	1.4304	0.5946
		970	0.0019	0.0756	1.4319	0.5768
		1922	0.0042	0.0767	1.4191	0.5655
		4002	0.0069	0.0766	1.4095	0.5605

Table 19. Percent Difference between 20 Point Spatial Resolution and 40 Point Spatial Resolution for the Lunar Habitat, Airlock.

Model	Target Point	# of Rays	Percent Error GCR-Dose	Percent Error GCR-Dose Equiv.	Percent Error SPE-Dose	Percent Error SPE-Dose Equiv
Lunar Habitat	Left Airlock	512	0.0097	0.0037	0.8912	0.6545
		968	0.0089	0.0054	0.9266	0.6891
		970	0.0104	0.0029	0.9147	0.6786
		1922	0.0143	0.0001	0.8866	0.6523
		4002	0.0110	0.0007	0.8795	0.6476

Table 20. Percent Difference between 20 Point Spatial Resolution and 40 Point Spatial Resolution for the Lunar Habitat, Crew Quarters.

Model	Target Point	# of Rays	Percent Error GCR-Dose	Percent Error GCR-Dose Equiv.	Percent Error SPE-Dose	Percent Error SPE-Dose Equiv
Lunar Habitat	Quarters	512	0.0488	0.1064	0.4995	0.5856
		968	0.0491	0.1078	0.5045	0.5880
		970	0.0452	0.1103	0.5077	0.5921
		1922	0.0512	0.1130	0.5111	0.5958
		4002	0.0529	0.1164	0.5190	0.6055